Available online at www.sciencedirect.com

ScienceDirect

00 (2019) 000–000

47th SME North American Manufacturing Research Conference, NAMRC 47, Pennsylvania, USA

A Framework for Optimizing Process Parameters in Powder Bed Fusion (PBF) Process Using Artificial Neural Network (ANN)

Mallikharjun Marrey[a], Ehsan Malekipour[a,*], Hazim El-Mounayri[a], Eric J. Faierson[b]

[a]*Collaborative Additive Manufacturing Research Initiative (CAMRI), Purdue School of Engineering and Technology, Indianapolis, IN 46202, USA*
[b]*Quad City Manufacturing Laboratory-Western Illinois University, Rock Island, IL 61201, USA; efaierson@qcml.org*

Abstract

Powder bed fusion (PBF) process is a metal additive manufacturing process, which can build parts with any complexity from a wide range of metallic materials. Research in the PBF process predominantly focuses on the impact of a few parameters on the ultimate properties of the printed part. The lack of a systematic approach to optimizing the process parameters for a better performance of given material results in a sub-optimal process. This process needs a comprehensive study of all the influential parameters and their impact on the mechanical and microstructural properties of a fabricated part. Furthermore, there is a need to develop a quantitative system for mapping the material properties and process parameters with the ultimate quality of the fabricated part to achieve improvement in the manufacturing cycle as well as the quality of the final part produced by the PBF process. To address the aforementioned challenges, this research proposes a framework to optimize the process for 316L stainless steel material. This framework characterizes the influence of process parameters on the microstructure and mechanical properties of the fabricated part using a series of experiments. These experiments study the significance of process parameters and their variance as well as study the microstructure and mechanical properties of fabricated parts by conducting tensile, impact, hardness, surface roughness, and densification tests, and ultimately obtain the optimum range of parameters. This would result in a more complete understanding of the correlation between process parameters and part quality. Furthermore, these experiments provide the required data needed to develop an Artificial Neural Network (ANN) model to optimize process parameters (for achieving the desired properties) and estimate fabrication time.

Keywords: Additive manufacturing; selective laser sintering; DMLS; artificial neural network (ANN); optimization framework; parameter optimization; sensitivity analysis

1. Introduction

PBF process is the most widely used additive manufacturing technology for metal printing and functional parts [1]. A wide range of metallic powder can be used as raw material for this process [2]. As with any other additive technology, PBF fabricates parts directly from 3D CAD data (STL file) and eliminates the use of expensive tooling [3, 4]. STL file slices the overall part into many layers with respect to the layer thickness and a laser beam sinters/melts each layer. Selective laser melting (SLM) and selective laser sintering (SLS) are the main two PBF processes. Unlike the SLM process, where the powder is completely melted down to form a homogeneous part, the SLS process partially melts the material (sinter the powder) layer-by-layer at the molecular level [5]. The schematic diagram in Fig. 1 shows the overall process of the PBF process [6]. The 3D printer machine consists of a supply station for the metal powder and a sintering/melting unit. A laser selectively sinters/melts the powder with respect to the layer geometry along a prescribed pattern. After sintering/melting of a layer, the powder dispenser platform moves upward a distance equals to the thickness of a layer to supply the material required for printing a new layer and a recoater arm or a roller transfers the material powder to the sintering/melting zone. The same process continues until the fabrication of the last layer [7].

Due to the ability of the PBF process to produce homogeneous parts with high strength alloys and allowable free-form fabrication [4], it has found applications in various sectors such as aerospace, defence, medical etc. [8, 9]. Aerospace industry widely employs the PBF process because of advantages such as timesaving and the ability to produce functional assemblies

* Corresponding author.
E-mail address: emalekip@purdue.edu (Ehsan Malekipour).

Marrey, M., Malekipour, E., El-Mounayri, H., & J.Faierson, E. (2019). A Framework for Optimizing Process Parameters in Powder Bed Fusion (PBF) Process Using Artificial Neural Network (ANN). Manuscript submitted for publication. Retrieved from https://easychair.org/publications/preprint/NXzq

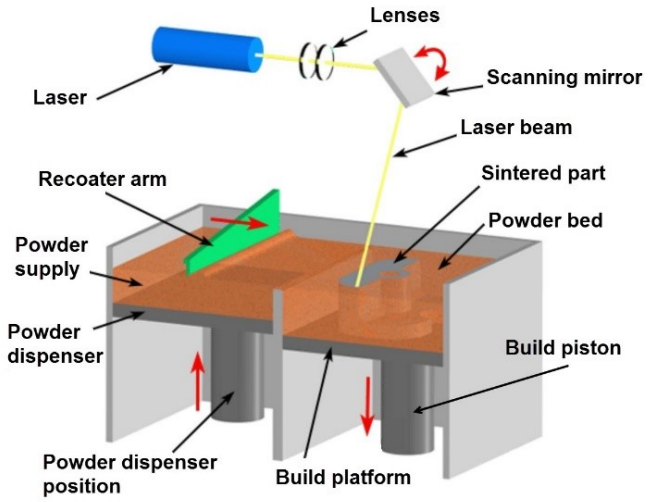

Fig. 1. A schematic diagram of direct metal laser sintering (DMLS) process [6]

[8, 10]. A wide range of metals such as Inconel 625, Inconel 718, 316L stainless steel, cobalt chrome, aluminum, titanium, and many alloys including Ti-6Al-4V are excellent materials for the aerospace industry, which are offering a significant cost and weight reduction [11, 12].

The PBF process has been employed in various industries however it still suffers from some process drawbacks. To overcome these drawbacks, the research in the PBF process nowadays concentrated on the impact detection of few parameters on the ultimate properties of the printed part [1, 5, 10, 13-18]. The ultimate goal is to develop a system linking manufacturing process, material properties, and the ultimate quality of a fabricated part to optimize the process parameters. Fulfilling this objective needs a comprehensive study on all the influential parameters with their significance on the mechanical and microstructural properties of a fabricated part. Furthermore, it needs to develop a quantitative system for mapping material property and process parameters to achieve improvement in the manufacturing cycle and quality control of the parts produced by the PBF process.

More than fifty parameters exist and have an influence on the ultimate quality of the product [19-21]. Scholars classify the process parameters into different groups [20, 22]. In one approach, Malekipour et al. [21, 22] classified the parameters into three main categories. The first category is pre-processed parameters including environmental conditions such as an inert gas, oxygen level, ambient temperature, powder specifications, and machine capabilities/limitations. The second category is the controllable parameters, which include process parameters, namely, laser specifications and scan strategy, and some few manufacturing specifications such as layer thickness. The last category includes the post-processed parameters, which quantify the ultimate quality of the fabricated part such as the yield strength, fatigue resistance, etc. [22]. Van Elsen named some of the important parameters in each classification. He mentioned that the powder specifications and deposition include morphology, the surface roughness of the generated grains, particle size distribution, and the deposition system of powder on to the bed. The laser specifications include spot size, wavelength, peak power, mode of the laser, and laser pulse length. The process parameters include part placement, scan strategy, build direction, laser power, scan speed, scan strategy, layer thickness, preheating temperature, hatch distance, and energy density [23].

The aforementioned parameters influence the process and the fabrication cost [20]. For instance, the process utilizes Argon instead of Helium as an environment for Ti-6Al-4V because Helium is 3 to 4 times more expensive than Argon [23]. However, previous literature shows that among all the factors affecting the PBF part few parameters, namely, laser power, scan speed, hatch spacing, layer thickness, beam diameter, and preheating temperature have a tremendous impact on mechanical efficiency, economy, and ultimate quality of the entire PBF process [5, 9, 18, 24].

The objectives of the study are first, to determine the optimal range of the process parameters and the way that different parameters affect the microstructure, densification, and mechanical properties of the printed part. Second, to specify the sensitivity of different parameters and identify which ones affect the overall performance the most, within the optimal range. Third, to optimize these parameters to be able to print a part with a better ultimate quality; and finally, to develop a system for quality control, and an intelligent network for suggesting optimized process parameters.

2. The current state of knowledge and gaps

Although PBF technology has significantly developed and is employed in different industries, many challenges and issues still remain. These challenges hinder the process repeatability, consistency, and stability of the process. Several research works have studied the influence of process parameters on quality for different materials and machines; however, it has proven very difficult to control all aspects of the process or evaluate the collective influence of all the parameters on the properties of a fabricated part.

Some previous work studied the effect of different process parameters on the ultimate surface quality. Yasa et al. [2] studied the staircase effect for nickel-based alloy parts manufactured by the SLS process. This research took the total waviness as the objective function and developed a predictive model. This model considered a few process parameters to develop it. Related to this work, Arasu et al. [1] and Hanzl et al. [3] studied the surface roughness of a part printed by the SLS process and conducted Analysis of Variance (ANOVA) to obtain the optimal parameter settings to achieve a better final surface finish. Similarly, Read et al. [25] used the response surface method to analyze various process parameters statistically and developed optimal parameters for surface roughness. This method has the advantage to consider a greater number of process parameters and conduct statistical analysis with a smaller number of experiments to print. Furthermore, Fox et al. [14] studied the effect of the process parameters on the surface roughness of overhanging structures in a powder-bed fusion process. This work covers a range of overhang angles and process parameters to determine a

relationship between process parameters, the angle of the overhanging surface, and the surface roughness.

There is more research, which focused on other aspects of the process. Sufiiarov et al. [26] studied the effect of the layer thickness on the parts printed by the SLM process. This study found that the microstructure, tensile strength, and elongation at the break depending on the layer thickness. Asgari et al. [9] used different process parameters available in an SLS system, such as laser power, scan speed, hatch distance, and laser offset distance for three different AlSi10Mg samples in 200 C with different surface roughness levels. This work employed Optical Microscopy (OM) and Scanning Electron Microscopy (SEM) techniques to study the microstructure of the printed samples. Moreover, Elsen [23] developed a genetic algorithm to perform variance analysis to study the complexity of the SLM process for a limited number of process parameters. The proposed methodology presented the synergistic possibilities of the mass-spring-damper system to optimize the density of fabricated parts by varying the selected parameters.

Konecna et al. [17] printed Ti-6Al-4V specimens by the SLM process in different orientations to determine the crack propagation and presented a stress intensity threshold for the growth of long cracks. In another study, Zhao et al. [27] evaluated the heat transfer and residual stress evolution in the parts produced by the SLS process and developed a numerical model by using COSMOL multi-physics environment for Ti6Al-4V. This study performed a thermo-mechanical simulation to study the change of residual stresses of a single layer, and physics and temperature of melt pool, which give a clear understanding of the thermo-mechanical evolution of a PBF additive process.

Hofland et al. [28] studied the mechanical properties of PA12 parts printed by the SLS process. In this work, they printed 480 tensile samples with 17 different sets of the process parameter. The part properties selected as output are tensile strength, tensile modulus, elongation at the break, and part density. Monte Carlo performed a simulation to determine the linear correlation between the coefficients and the sensitivities of the process parameters. This simulation derived some interesting parameters properties, which influence the ultimate mechanical properties of the printed parts. Finally, Munguia et al. [29] employed a neural network-based model for the estimation of the build time in the SLS process as well as a MATLAB simulation to validate the results with the existing cost estimation models.

However, these research studies focused on identifying the influence of few process parameters, predominantly laser specifications, on the surface quality or selective mechanical properties of the printed part; limited research works studied the correlation between the parameters and the ultimate properties of the printed part. However, there is a lack of a consistent system considering/optimizing all the controllable parameters and mapping the process, material, and parameters onto the ultimate properties of the fabricated parts. Furthermore, Optimizing the machine setting by controlling the aforementioned parameters is a prerequisite for a near flawless fabrication process. The ultimate contribution of this work is to examine the effect of a set of parameters instead of the effect of their individual impact on the selected properties of a fabricated part. This will help

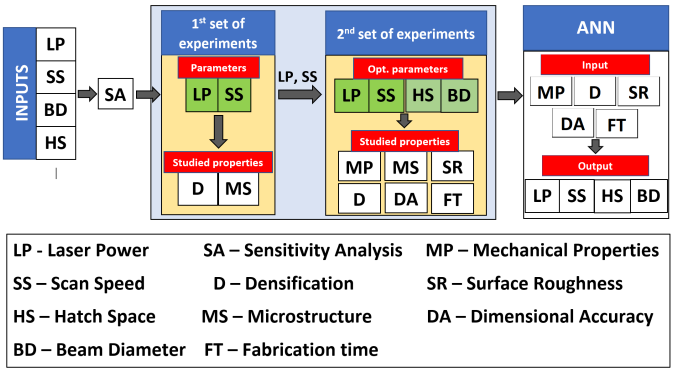

Fig. 2. Proposed framework and corresponding workflow for developing ANN model

to fill the existing gap for development of a standardized system, which maps all the contributing and controllable process parameters and material specifications onto the ultimate quality of fabricated parts. Furthermore, manufacturers can employ this system to ensure full compliance with the customers demands.

This paper first, provides a two-step framework toward this ultimate objective. Second, it yields the results, which employ the microstructure and porosity in order to narrow down the working energy density for near-full densification (see section 4). We will conduct the experiments in the second step within the optimized range of the laser power and scan speed obtained in the first step. The latter step, for the first time, will study the effects of altering laser power, scan speed, hatch space, and beam diameter all together on ultimate quality of a printed part and map them together (see Fig. 2). The significance of this study versus the previous literature is first, we study the effects of a set of four parameters on the ultimate quality of a fabricated part (and not just one parameter or two). Second, we consider the effects of these parameters on the fabrication time and various aspects of the ultimate quality of a fabricated part, including microstructure, densification, mechanical properties, dimensional accuracy, and surface roughness. Finally, we employ the results to train a feed-forward back-propagation (FFBP) neural network (NN). The function will suggest the optimized parameters according to the desired ultimate quality of an ordered part.

3. Research methodology

Researchers have been studying the influence of every contributing parameter on the ultimate properties of a fabricated product. However, a collective system, which considers all the controllable parameters, is missed. The framework introduced in this paper will help in achieving a comprehensive understanding of the process and the importance of each parameter as well as obtaining the optimal range of significant parameters such as laser power, scan speed, hatch spacing, and beam diameter in the manufacturing process. As Fig. 2 shows, first, we select the parameters according to the prioritized and influential order cited in the literature [21, 28] and then, this system conducts the Sensitive Analysis (SA) to figure out the importance

of each individual parameters from the selected ones setting up the levels for next step. Then, this system conducts two sets of Design of Experiments (DOE) in the next steps and tests the consequent properties of the fabricated parts. The system will finally employ the acquired results to train an intelligent system suggesting the optimized process parameters for obtaining a better ultimate quality as well as estimating fabrication time of the parts printed by the PBF process with the Ti-6Al-4V material. The following sections explain the details of the proposed framework.

3.1. Material properties

316L stainless steel is the material considered for this research. The alloy composition and actual specifications as supplied are shown in Table 1. 316L SS has widespread application in additive manufacturing due to its good tensile strength at high temperatures, low stress to rupture, high hardness, toughness and corrosion resistance properties [30].

3.2. Design of specimen

This work employs the ASTM E8 standard specimen (Table 3) [31] to test the tensile properties. We extend the specimen length on both sides to perform more mechanical testing, namely, hardness, and impact as well as to study the microstructure more. The quality and precision of the specimens are vital to get some more accurate metallographic analysis.

Fig. 3 shows the designed specimen, which includes three sections for the tensile testing specimen (the middle section), the impact test (the left section), and the hardness test (the right section) of the specimen. All the dimensions are modified according to the ASTM standards.

3.3. Sensitivity analysis

Sensitivity analysis (SA) quantifies the correlation between the given model and its input parameters [32]. The main objective of conducting SA are to understand (1) which parameters require additional research for strengthening the knowledge base, thereby reducing output uncertainty; (2) which parameters are irrelevant and can be eliminated from the final model; (3) which inputs contribute most to output variability; and (4) which parameters are most highly correlated with the output [32].

Table 1. Composition of 316L SS [33]

Grade 316L	Min	Max	Actual
Carbon, C	-	0.03%	0.019%
Silicon, Si	-	0.75%	0.67%
Manganese,Mn	0.03%	<0.1%	<0.08%
Phosphorus, P	-	<0.025%	<0.019%
Sulphur, S	-	<0.01%	<0.006%
Chromium, Cr	17.5%	<18%	<17.9%
Nickel, Ni	12.5%	<13%	<12.7%
Molybdenum, Mo	2.25%	<2.5%	<2.36%
Nitrogen, N	-	<0.1%	<0.06%
Copper, Cu	-	<0.5%	<0.2%
Oxygen, O	-	<0.1%	<0.022%
Iron, Fe	Balance	Balance	Balance

Table 2. Tensile testing specimen, ASTM E8/E8M 13a [31]

Dimensions for the subsize specimen (6 mm [0.250 in.] wide) (mm [in.])	
G Gauge length	25.0 0.1 [1.000 0.003]
W Width	6.0 0.1 [0.250 0.005]
T Thickness	Maximum 6 mm
R Radius of fillet, min	6 [0.250]
L Overall length, min	100 [4]
A Length of reduced section, min	32 [1.25]
B Length of grip section, min	30 [1.25]
C- Width of grip section, approximate	10 [0.375]

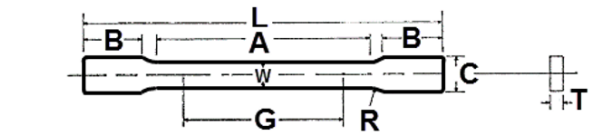

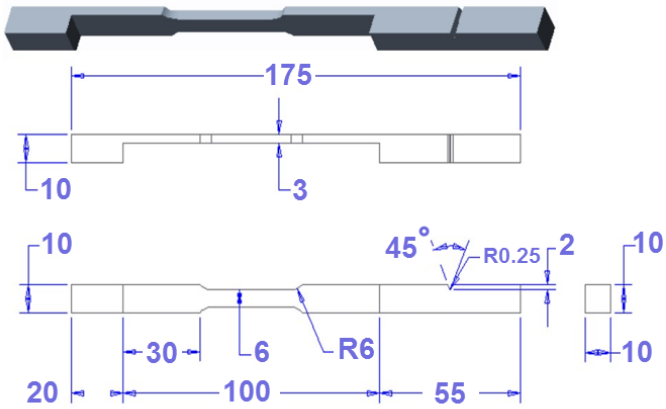

Fig. 3. Designed specimen

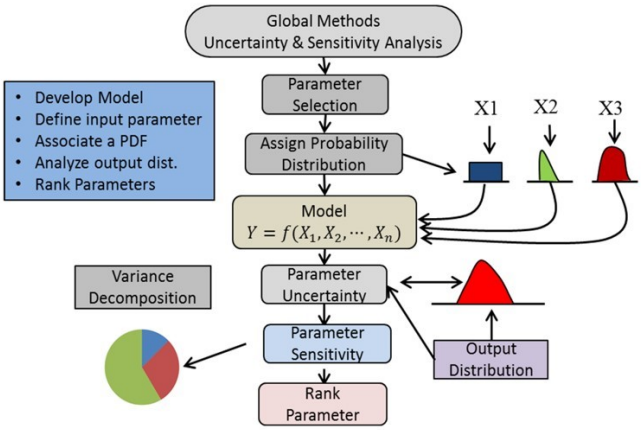

Fig. 4. Schematic for global sensitive analysis [34]

The laser power, scan speed, layer thickness, beam diameter, and the hatch spacing are commonly cited in the literature as the crucial controllable parameters in the DMLS process influencing the ultimate quality of the fabricated part [21, 28]. SA considers these five parameters to evaluate their correlation with the volume based energy density (ED) shown in equation (1) [35]. However,the employment of SA is crucial to demonstrate the sensitivity of each parameter within the working range in this work. The sensitivity analysis guides us through selecting the levels of parameters and their distribution for designing the experiments during the next step.

$$ED = \frac{P}{S * V * t} \tag{1}$$

where P is laser power, S is hatch spacing, V is scan speed, and t is layer thickness, which is set to a constant value of 30 μm in this research. Fig. 4 shows the schematic process of global SA employed by MATLAB [36]. The SA results evidently show the scan speed as the most sensitive parameter, which drastically changes the energy applied per volume and might influence the ultimate properties of the fabricated part predominantly [35]. In a similar way, the laser power and hatch spacing also have a considerable effect. The effect of layer thickness is not calculated as it is set to a constant value throughout this research. Fig. 5 shows the values of the total global sensitivity coefficient obtained by SA.

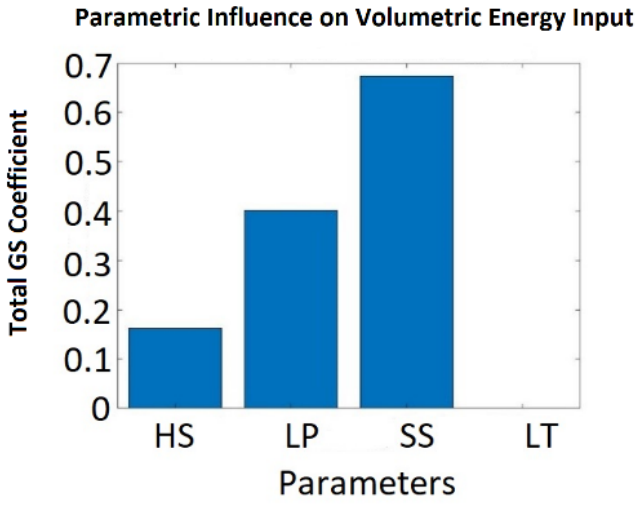

Fig. 5. Total Global Sensitivity (GS) Coefficient

Previous literature also confirmed the significant influence of laser power and scan speed, as two main parameters that affect the energy transferred to the powder, on the ultimate quality of the printed part. D. Gu and Y. Shen [8] conducted experiments with different combination values of laser power and scan speed on stainless steel 316L with the layer thickness of 20 μm. Their study shows the parameters generates four different melting status shown in Fig. 6.

In case I, which is called the no-melting zone, the energy density is insufficient to melt the powder leaving the powder

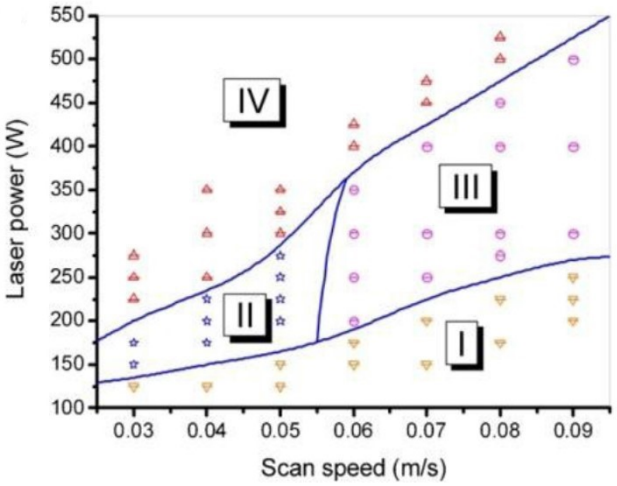

Fig. 6. The dependency of structure on procedural parameters [8]

in its initial state. In case II, a medium laser power scans the powder with a low scan speed leading to the partially melted powder. This phase forms coarsened balls after crystallization, which is the first form of the balling phenomenon. A high laser power and high scan speed melt the powder with balling phenomenon along the scanned pattern in the form of thin cylindrical lines in case III. Complete melting occurs in the case of IV as the high laser power forms a solid surface by continuous lines of fully melted powder along the scan paths.

3.4. Design of experiments

In this research, there are two sets of experiments in order to obtain the optimized process parameters for a PBF machine with laser power less than 200 W. The first set of experiments employs full factorial analysis method due to the limited number of experiments. Table 3 shows the parameters, namely, the laser power and scan speed, whose values are assigned based on the literature [13, 26, 35]. The first set of experiments prints a $10mm \times 10mm \times 5mm$ samples considering merely the laser power and scan speed, while hatch spacing and beam diameter are kept fix at their machine default values. The layer thickness is also set to a constant value of 30μm throughout the work. In this phase, we study the microstructure, porosity, and densification of the printed samples to map them onto the energy density. Previous literature demonstrated that the porosity generated in the microstructure of a printed part significantly affects the mechanical properties of a fabricated part. The porosity change in low ranges (near full density parts) is seen to alter mechanical properties substantially [37]. Moreover, reducing the porosity enhances the build consistency [38]. Thus in this phase, we seek to obtain the optimal range of energy density for maximum densification. It should be noticed that we study only 13 samples due to very close energy density for four of the samples.

Taguchi method designs the second set of experiments considering the optimum range of energy density and the number of levels obtained from the first set. This phase derives the op-

Table 3. Control factors and levels for DOE

Factor	Level values	Levels
Laser Power, W	100, 125, 150, 175	4
Scan Speed, *mm/sec*	600, 800, 1000, 1200	4

timum values for the selected set of process parameters, which have a decisive impact on the ultimate properties of a fabricated part. To do so, we will conduct 64 experiments (L64 OA), selected by Taguchi method, and study the effect of the laser power, scan speed, beam diameter, and hatch spacing on the ultimate quality of printed samples (see Fig. 2).. Taguchi method is a statistical method, which designs experiments using Orthogonal Array (OA) technique to improve the quality of a manufacturing process [23]. The OA technique converts the parameter design values to S/N ratio and calculates the design robustness [15]. To improve the product quality, the quality characteristics must deviate as little as possible from the target value. OA is a systematic and statistical way of testing interactions between control factors. It provides a uniformly distributed set of experiments, which covers all the paired combinations of the variables [39] instead of the full factorial analysis (256 number of experiments in this case), which is unnecessary because it requires a significant amount of material to and a great deal of time to fabricate numerous specimens. Fig. 3 shows the designed sample for running the second set of experiments. The results and data acquired from the second set will eventually be employed in developing ANN.

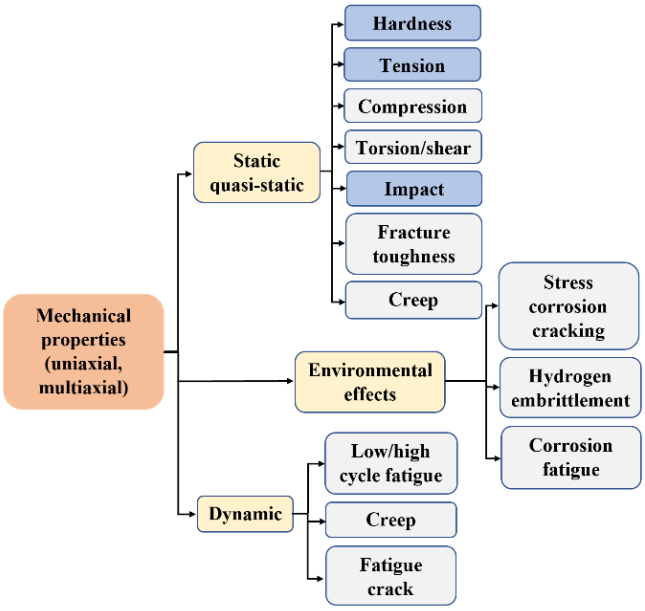

Fig. 7. Mechanical properties summary

3.5. Mechanical properties

As Fig. 7 shows, a series of tests measure the mechanical properties and characteristics of the printed samples acquired by DOE. Various mechanical tests, namely, tensile, hardness, and impact investigate the mechanical characteristics of the fabricated product including surface finish, residual stresses, porosity, microstructure, and densification. The first set of samples studies the effect of a limited number of process parameters, namely, laser power and scan speed on the microstructure, porosity and density values for the samples printed by Ti-6Al-4V, using SEM and Archimedes principle. The second set studies the aforementioned mechanical properties of the printed samples to optimize a wider range of process parameters.

ANOVA employs the data acquired from the previous sets of experiments for data analysis, variance analysis, and ultimately helps in designing the Neural Network (NN) with the capability of intelligent suggestion of the process parameters. The next section provides more details about this approach.

3.6. Data analysis

3.6.1. Signal/noise ratio and analysis of variance (ANOVA)

The signal/noise (S/N) is a method of variability measurement of the manufacturing process, which evaluates the process parameters at all individual levels and ensures the resulting optimum process conditions are robust and stable. The following equations calculate three types of S/N ratios, namely, the lower-the-better used for surface roughness (Eq. 2), the higher-the-better used for mechanical properties (Eq. 3), and the nominal the better used for dimension accuracy (Eq. 4) [15, 25].

$$\frac{S}{N} = -10 * log_{10}\left(\frac{1}{n}\sum_{i=1}^{n} Y_i^2\right) \tag{2}$$

$$\frac{S}{N} = -10 * log_{10}\left(\frac{1}{n}\sum_{i=1}^{n} \frac{1}{Y_i^2}\right) \tag{3}$$

$$\frac{S}{N} = -10 * log_{10}(s^2) \tag{4}$$

where n is the number of measurements and Y_i is the observed performance characteristic value and s is the standard deviation of the responses for the given factor level combination.

S/N value will be calculated in the second set of experiments (64). With the factor of having 64 experiments, even the slightest variation/error in employing S/N value can be identified when the resulting S/N values will be used for calculating the variance. After the calculation of S/N value, a method called Analysis of Variance (ANOVA) statistically evaluates the significance of the control factors (i.e. process parameters in our work) and their influence on the experimental results (mechanical properties). ANOVA studies the variance of properties with the levels of parameters by employing the data available after material and mechanical testing [39]. The provided graphs and distribution charts will describe the variance of properties within the tested range of levels; thus, they will obtain the optimal range of the values for Ti-6Al-4V in the PBF process. This will complete the correlation between the material and process-properties for the PBF process, which will guide in the development of an ANN system.

4. Results and discussion

We cut each of the samples in the first set of experiments from the center in both directions, namely, perpendicular to the build direction and parallel to the build direction (see Fig. 8) by using electric discharge machining (WEDM) process.

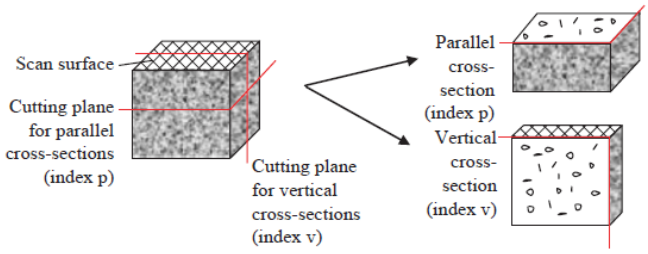

Fig. 8. Cutting planes in the specimens of the first set [40]

We take sixteen micrographs in total from each sample by using a scanning electron microscope (SEM). Six micrographs are taken from the horizontal cross-section (each corner plus two from the center area) and two from the vertical one (Fig. 9), each uses two different magnifications i.e. 60X and 300X (100μm and 10μm scale respectively (see Fig. 4 for an instance)). We employ the MATLAB image processing to measure the porosity of each sample in two steps (Fig. 3). First, MATLAB creates black and white (BW) images from the micrographs. In these images, the black pixels represent the porosity and the white pixels represent the solid. In this step, the threshold level is adjusted by comparing the pore size in the SEM image (Fig. 10.a) with the image generated by MATLAB (Fig. 10.b) to increase the accuracy of the method [41]. Then, we calculate the ratio of the number of black pixels to the total pixels for the horizontal BW micrographs and the vertical ones

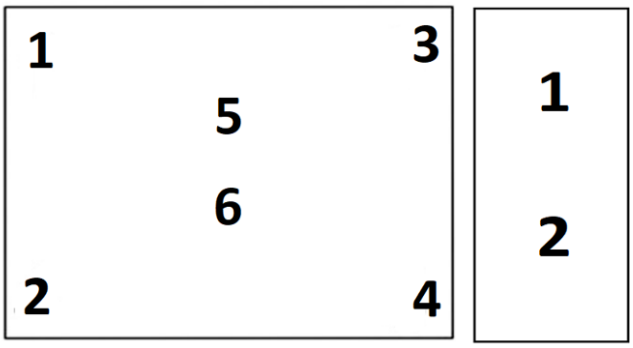

Fig. 9. The position of the images captured from (a) horizontal (b) vertical cross-section

separately. The overall average ratio for both magnifications on the BW images of horizontal cross-section and vertical cross-sections represent the porosity value of the printed sample in each direction.

The horizontal cross-section micrographs of the samples from the first set of experiments show the energy densities applied to the samples generate three different types of porosity

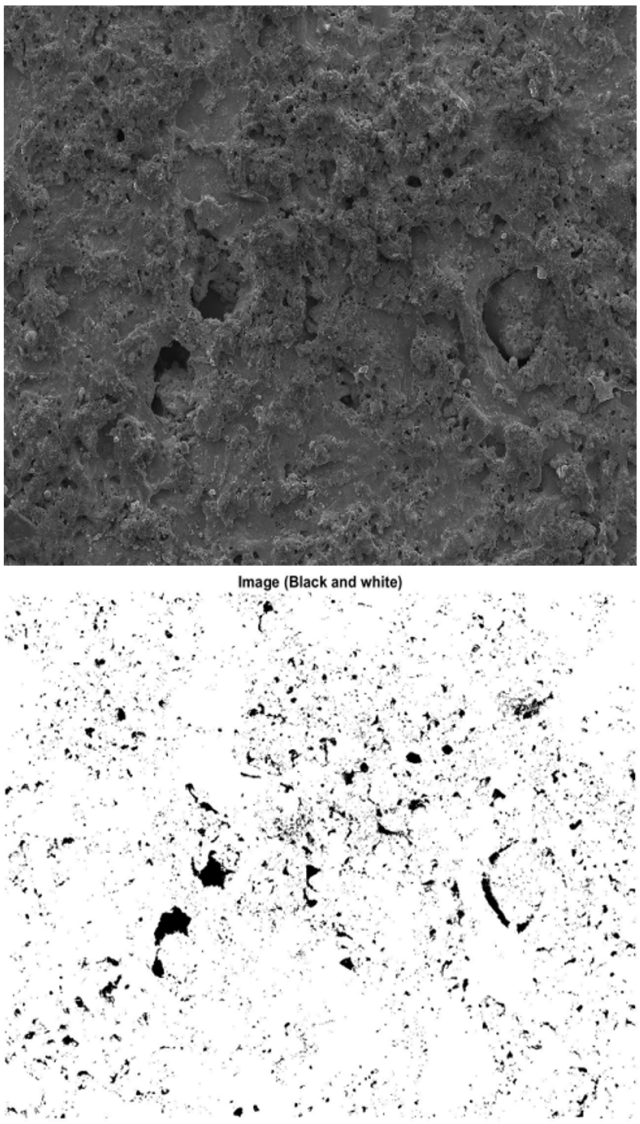

Fig. 10. (a) SEM image and (b) MATLAB image

according to low, medium, or high value of volumetric energy density (VED). Low volumetric energy density leads to incomplete melting of the powder particles and formation of irregular pores due to lack of fusion such as sample 3 (the low VED with LP 100 W and SS 900 mm/s) (Fig. 11.a). While, the exertion of high volumetric energy vaporizes the material and hence, it leads to the formation of circular gas pores such as sample 13 (the highest VED with LP 175 W and SS 700 mm/s) (Fig. 11.b). These circles can be a cross-section for a keyhole porosity. Samples with medium VED such as sample 16 (medium VED with LP 175 W and SS 1000 mm/s) possess microscale holes with a nearly uniform distribution throughout the cross-section, which is an evidence in better mechanical properties compared with the other types [42]. Table 4 illustrates the porosity values of the three aforementioned samples. The results are confidently in agreement with the results from the previous literature

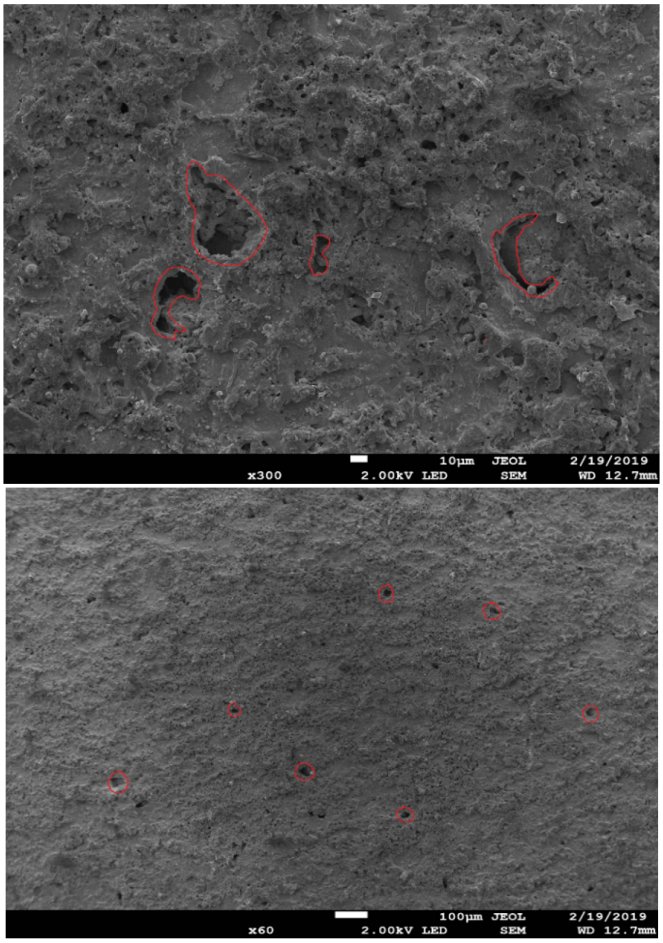

Fig. 11. Different pores formed during the process (a) Lack-of-fusion pores (b) Gas pores

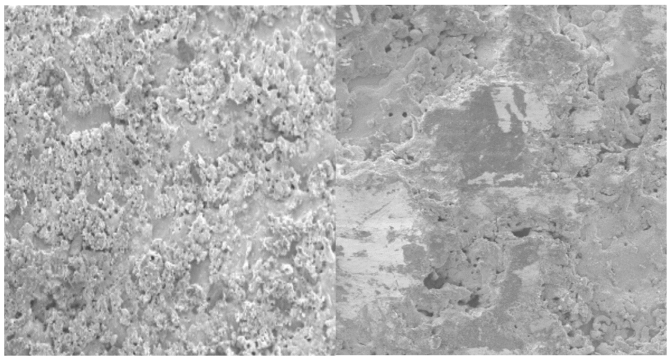

Fig. 12. Horizontal vs vertical cross-section SEM images

such as cherry et. Al. [33]. Different types of porosity are visible in horizontal and vertical cross sections, which lead to different porosity percentage in each cross section. Vertical cross sections illustrate the less frequent but bigger size porosity usually progressing through layers. Whereas, horizontal cross sections illustrate the widespread porosity in different size ranges, which scatters throughout the entire section (Fig. 12). The average porosity will be used in the future phase of this framework.

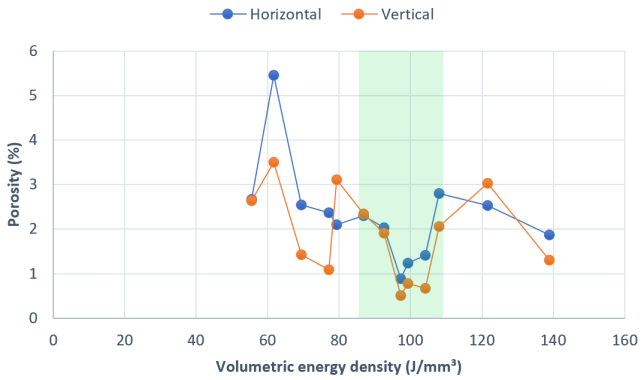

Fig. 13. Porosity vs VED for first set of experiments

Table 4. Porosity of the samples

Sample no.	Horizontal (%)	Vertical (%)	Average porosity
3, VED = 61.7 J/mm^3	5.453	3.5	4.48
16, VED = 97.2 J/mm^3	0.8793	0.502	0.69
13, VED = 138 J/mm^3	1.8736	1.308	1.59

The porosities in horizontal and vertical cross-sections for the samples according to the applied VED is shown in Fig.12. As Fig. 13 shows, the energy density alters between 55 and 138 J/mm^3. This energy density creates a part with the density between 95.52% and 99.31% with a maximum of 99.31%. The maximum density is achieved with the VED of 99.2 and 104.17 J/mm^3. Considering the densification percentage, we can narrow down the range of optimum VED to 85 J/mm^3 and 110 J/mm^3. This range of VED suggests the optimized range between 150 W to 200 W for the laser power and 800 mm/s to 1000 mm/s for scan speed to obtain the maximum densification. These ranges will be employed as the inputs for the second phase (second set of experiments) in the framework. The second set will map the set of four process parameters into the ultimate characteristics of a printed part.

5. Future Work: Neural Network method

There are two main methods for modeling a manufacturing process. First, a physics-based and second, a data-driven modeling. The physics-based modeling technique analyzes a manufacturing process from a physical point of view. However, this traditional analytical modeling method is not always suitable to model some modern complex manufacturing processes, such as AM, due to the number of process variables and the non-linear complex nature of the process.

Another modeling method is empirical modeling, which employs experimental data and statistical theory [39]. Many applications in manufacturing engineering successfully implemented the ANN methodology as a good empirical modeling method. This work employs the acquired data from the experimental sets, explained in the previous sections, to model the process by creating a correlation function between the process

parameters and ultimate properties of the fabricated parts. This function helps in adjusting the process parameters in order to fabricate parts in accordance with the users desired requirements, namely, mechanical properties, microstructure, fabrication time, dimensional accuracy, and surface roughness. The aforementioned qualities may have an adversarial nature or effects on each other. Thus, providing a guideline to control them through the selection of the process parameters seems crucial. Numerous literature such as [1-4, 21-25] demonstrates the contributing factors to the ultimate qualities and studied the correlation between them. For instance, Malekipour et al. [22] classified the process parameters according with their correlation with the defects generated during the powder-bed fusion (PBF) process. The results demonstrated that laser specifications, namely, laser power, scan speed, hatch space, and beam diameter are the most effective parameters contributed to the defects during the PBF processes. Moreover, this current paper employs SA to demonstrate the influence of every single parameter within a set of parameters on a selected ultimate quality. However, no literature neither has investigated the influence of the set of these parameters simultaneously on the ultimate qualities of a fabricated part nor has considered all the aforementioned ultimate qualities for developing an optimization model. These two gaps are highly in demand and can be achieved by the employment of ANN for the PBF process.

This study is employing a feed-forward NN, which adopts the back-propagation (BP) algorithm to develop a multiple input/output optimization models. The inputs include the process parameters (laser power, scan speed, hatch space, and beam diameter) while the outputs include ultimate properties of a fabricated part (densification, mechanical properties, surface roughness, dimensional accuracy, and fabrication time) (see Fig. 14). Development of this multi-input/output ANN function will eventually lead to an intelligent system capable of controlling multiple parameters simultaneously.

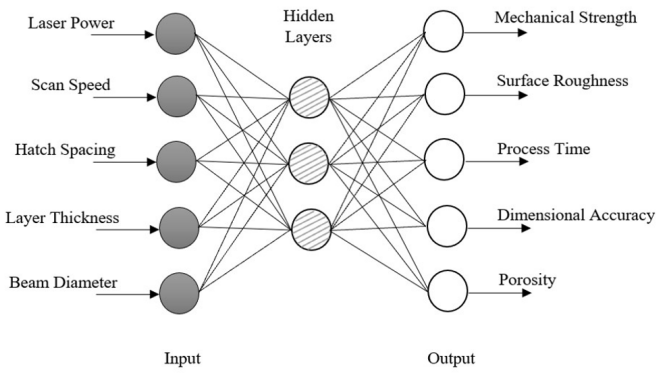

Fig. 14. The schematic ANN architecture of this research

The framework presented in this work employs two sets of experiments to first, narrow down the process parameters (the inputs) to their optimized ranges and second, study how a set of parameters contribute to the ultimate properties (the outputs). This data is essential for building the necessary database to develop this multiple input/output optimization models. Employment of plentiful data to train an NN function with high accuracy is crucial. First, this work considers 16 full factorial experiments to find the optimized range of laser power and scan speed to fabricate parts with a nearly full density during the first set of experiments (see subsection 3.4). This set does not use ANN for optimization, but rather it employs a MATLAB code to measure the density of the printed samples one-by-one according to the images taken by scanning electron microscopes (SEM). However, the second set is employing ANN to acquire the optimum ranges of the input parameters. In this case, we profit from Taguchi method to select and print 64 samples with a various range of parameters. Furthermore, we are studying the accuracy of employment of generative adversary network (GAN) in order to generate a sufficient number of inputs for training the function by ANN. The trained function can be customized even further according with the necessities and unique product of each company.

We will start designing the feed-forward NN with one hidden layer and traingdx training algorithm with by using MATLAB deep learning toolbox. The number of iterations is set to a maximum of 10000, the performance goal is set to 0 according with the mean square error (MSE), and the other training parameters are set to their default values. The best approximation with the least MSE specifies the best network topology. BP algorithm calculates and adjusts the weights, which gradually brings the output closer to the required output.

This system will go towards a comprehensive control system in the PBF process within two steps. First, we develop a NN intelligent system, which makes users/manufacturers capable of selecting the process parameters according with the required/desired ultimate properties of a fabricated part (the current project) (Fig. 15). Second, we integrate this system with an online monitoring and control (OMC) system to fabricate nearly flawless parts with the desired ultimate qualities (the long-term objective). Plentiful research nowadays has focused on the development of OMC systems [43-48] to avoid/diminish the defects and abnormalities generated during the fabrication process [21, 22, 49-52]. Monitoring and control of the thermal specifications and thermal evolution of any inherently thermal AM process has been recognized as a crucial step towards improving the microstructure and ultimate mechanical properties of a fabricated part [53-55]. Nowadays, most vendors try to handle the frequent thermal anomalies of the fabricated parts such as distortion by designing some temporary support structures. These supports facilitate the conduction during the fabrication process and strengthen the structure.

Designing the topology-optimized support structures reduces the fabrication time and material [56] however the fabricated parts still need a significant work for post-processing. Optimization of process parameters by using an ANN model in this project integrated with an OMC system can considerably improve the mechanical properties and surface quality of fabricated parts, increase the repeatability, reduce fabrication time, and significantly decrease the need for the post-processing operations.

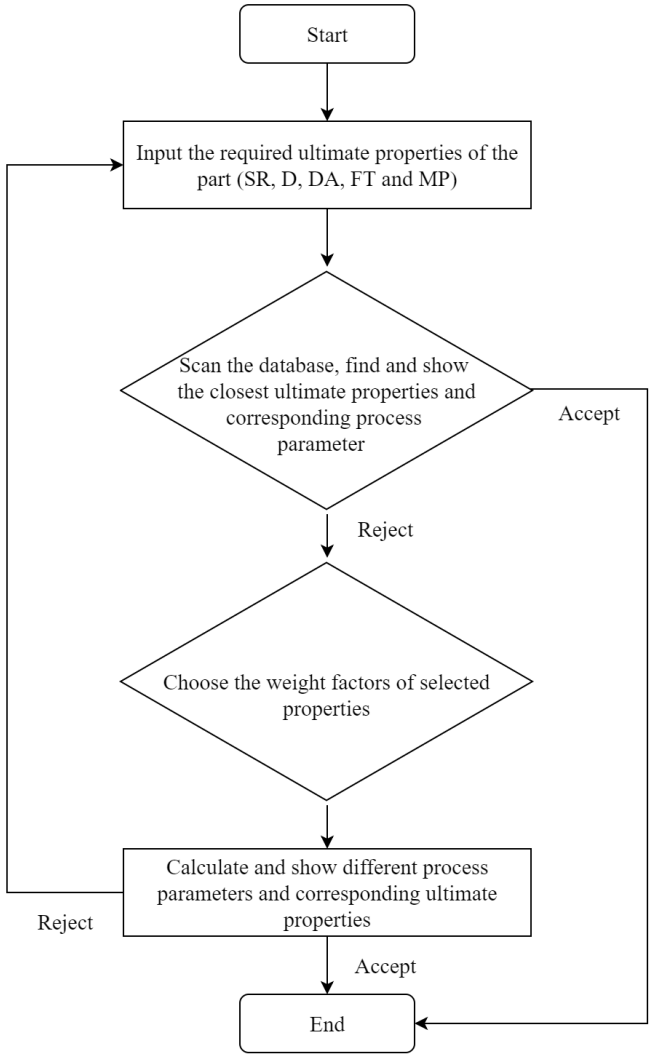

Fig. 15. The algorithm of selection process parameters [57]

6. Conclusion

This study presents a framework for optimization of the PBF process by mapping the ultimate quality of a fabricated part into the process parameters and material properties. The first phase studies the effects of laser power and scan speed on the microstructure and porosity of SS 316L fabricated parts. To do so, it studies the energy density between 55 and 138 J/mm3 and demonstrates that the porosity alters between 0.69% to 4.48%. The near-fully densification of 99.31% with a uniform microstructure is achieved for energy density equals to 97.2 J/mm3. The results suggest that the optimum range of energy density is between 85 J/mm3 and 110 J/mm3 to achieve maximum densification. Furthermore, this phase measures the influence and sensitiveness of laser power, scan speed, hatch spacing, and beam diameter within the optimal range. The results show that the energy density is sensitive to scan speed more than other parameters within the optimal range.

The second phase of this framework leverages the acquired data from the first phase to correlate the parameters with the mechanical properties, residual stresses, surface roughness, dimensional accuracy, and microstructure development. This correlation will help in the development of an intelligent neural network for parameter suggestion and build-time estimations.

Further steps introduced in the second phase have to be taken to eventually create a mapping between process, parameters, and ultimate quality properties of a fabricated part.

7. Acknowledgement

We appreciate CAMRI Research Laboratory that supported this research. We would also like to show our gratitude to our colleagues from the Quad City Manufacturing Laboratory, who provided insight, expertise, and facilities for the experimental studies that greatly assisted the research, although they may not agree with all the interpretations/conclusions of this paper. We also appreciate Nojan Aliahmad for his valuable help in this work.

References

[1] Arasu, I., et al., Optimization of surface roughness in selective laser sintered stainless steel parts. Vol. 6. 2014. 2993-2999.
[2] Yasa, E., et al., A Study on the Stair Stepping Effect in Direct Metal Laser Sintering of a Nickel-based Superalloy. Procedia CIRP, 2016. 45: p. 175-178.
[3] Hanzl, P., et al., The Influence of Processing Parameters on the Mechanical Properties of SLM Parts. Vol. 100. 2015.
[4] Dingal, S., et al., The application of Taguchis method in the experimental investigation of the laser sintering process. Vol. 38. 2008. 904-914.
[5] Hardik Varia, B.G., A Review on Effect of Process Parameters on Surface Quality and Properties of Parts Realized by Selective Laser Sintering Process. International Journal on Recent and Innovation Trends in Computing and Communication (IJRITCC), 2017: p. 45-51.
[6] Custompart.net: 'Direct Metal Laser Sintering'. [cited 2018 June 25]; Available from: http://www.custompartnet.com/wu/direct-metal-laser-sintering.
[7] Verma, A., P.S. Tyagi, and K. Yang, Modeling and optimization of direct metal laser sintering process. Vol. 77. 2014.
[8] Gu, D. and Y. Shen, Processing conditions and microstructural features of porous 316L stainless steel components by DMLS. Applied Surface Science, 2008. 255(5, Part 1): p. 1880-1887.
[9] Mohammadi, M. and H. Asgari, Achieving low surface roughness $AlSi10Mg_200C$ parts using direct metal laser sintering. Additive Manufacturing, 2018. 20: p. 23-32.
[10] Calignano, F., et al., Influence of process parameters on surface roughness of aluminum parts produced by DMLS. The International Journal of Advanced Manufacturing Technology, 2013. 67(9): p. 2743-2751.
[11] DMLS.com. DMLS applications. [cited 2018 10/01]; Available from: http://dmls.com/dmls-applications.
[12] Stratasys. Direct metal laser sintering materials. [cited 2018 10/01]; Available from: https://www.stratasysdirect.com/materials/direct-metal-laser-sintering.
[13] Gong, H., et al., Defect Morphology of Ti-6Al-4V Parts Fabricated by Selective Laser Melting and Electron Beam Melting. 2013.
[14] Fox, J.C., S.P. Moylan, and B.M. Lane, Effect of Process Parameters on the Surface Roughness of Overhanging Structures in Laser Powder Bed Fusion Additive Manufacturing. Procedia CIRP, 2016. 45: p. 131-134.
[15] Kumar, N., H. Kumar, and J.S. Khurmi, Experimental Investigation of Process Parameters for Rapid Prototyping Technique (Selective Laser Sintering) to Enhance the Part Quality of Prototype by Taguchi Method. Procedia Technology, 2016. 23: p. 352-360.

[16] Delgado, J., J. Ciurana, and C.A. Rodrguez, Influence of process parameters on part quality and mechanical properties for DMLS and SLM with iron-based materials. The International Journal of Advanced Manufacturing Technology, 2012. 60(5): p. 601-610.

[17] Konen, R., et al., Long Fatigue Crack Growth in Ti6Al4V Produced by Direct Metal Laser Sintering. Vol. 160. 2016. 69-76.

[18] Pal, S., et al., The Effect of Post-processing and Machining Process Parameters on Properties of Stainless Steel PH1 Product Produced by Direct Metal Laser Sintering. Vol. 149. 2016. 359-365.

[19] Yadroitsev, I., P. Bertrand, and I. Smurov, Parametric analysis of the selective laser melting process. Applied Surface Science, 2007. 253(19): p. 8064-8069.

[20] Spears, T.G. and S.A. Gold, In-process sensing in selective laser melting (SLM) additive manufacturing. Integrating Materials and Manufacturing Innovation, 2016. 5(1): p. 2.

[21] Malekipour, E. and H. El-Mounayri, Defects, Process Parameters and Signatures for Online Monitoring and Control in Powder-Based Additive Manufacturing, in Mechanics of Additive and Advanced Manufacturing, Volume 9. 2018, Springer. p. 83-90.

[22] Malekipour, E. and H. El-Mounayri, Common defects and contributing parameters in powder bed fusion AM process and their classification for online monitoring and control: a review. The International Journal of Advanced Manufacturing Technology, 2018. 95(1): p. 527-550.

[23] Van Elsen, M., Complexity of selective laser melting : a new optimisation approach. 2007.

[24] Ruban, W., et al., Effective process parameters in selective laser sintering. International Journal of Rapid Manufacturing, 2014. 4(2-4): p. 148-164.

[25] Read, N., et al., Selective laser melting of AlSi10Mg alloy: Process optimisation and mechanical properties development. Vol. 65. 2015. 417-424.

[26] Sufiiarov, V.S., et al., The Effect of Layer Thickness at Selective Laser Melting. Procedia Engineering, 2017. 174: p. 126-134.

[27] Zhao, X., et al., Numerical modeling of the thermal behavior and residual stress in the direct metal laser sintering process of titanium alloy products. Additive Manufacturing, 2017. 14: p. 126-136.

[28] C. Hofland, E., I. Baran, and D. Wismeijer, Correlation of Process Parameters with Mechanical Properties of Laser Sintered PA12 Parts. Vol. 2017. 2017. 1-11.

[29] Mungua, J., J. Ciurana, and C. Riba, Neural-network-based model for build-time estimation in selective laser sintering. Proceedings of the Institution of Mechanical Engineers, Part B: Journal of Engineering Manufacture, 2009. 223(8): p. 995-1003.

[30] DebRoy, T., et al., Additive manufacturing of metallic components Process, structure and properties. Progress in Materials Science, 2018. 92: p. 112-224.

[31] ASTM, Standard Test Methods for Tension Testing of Metallic Materials, in E8 / E8M - 13. 2013: ASTM International, West Conshohocken, PA.

[32] Hamby, D.M., A review of techniques for parameter sensitivity analysis of environmental models. Environmental Monitoring and Assessment, 1994. 32(2): p. 135-154.

[33] Cherry, J.A., et al., Investigation into the effect of process parameters on microstructural and physical properties of 316L stainless steel parts by selective laser melting. The International Journal of Advanced Manufacturing Technology, 2015. 76(5): p. 869-879.

[34] Nasir, B., Implementation of Sobols Method of Global Sensitivity Analysis to a Compressor Simulation Model, in 22nd International Compressor Engineering Conference. 2014, Purdue e-Pubs: Purdue.

[35] Thijs, L., et al., A study of the microstructural evolution during selective laser melting of Ti6Al4V. Acta Materialia, 2010. 58(9): p. 3303-3312.

[36] Pianosi, F., F. Sarrazin, and T. Wagener, A Matlab toolbox for Global Sensitivity Analysis. Environmental Modelling Software, 2015. 70: p. 80-85.

[37] Gangireddy, S., Gwalani, B., Liu, K., Faierson, E. J., Mishra, R. S. (2019). Microstructure and mechanical behavior of an additive manufactured (AM) WE43-Mg alloy. Additive Manufacturing, 26, 53-64.

[38] Palanivel, S., Dutt, A. K., Faierson, E. J., Mishra, R. S. (2016). Spatially dependent properties in a laser additive manufactured Ti6Al4V component. Materials Science and Engineering: A, 654, 39-52.

[39] Chen, H., A process modelling and parameters optimization and recommendation system for binder jetting additive manufacturing process, in Department of Mechanical Engineering 2016, McGill University: Montreal

[40] Spierings, A.B., M. Schneider, and R. Eggenberger, Comparison of density measurement techniques for additive manufactured metallic parts. 2011. 17(5): p. 380-386.

[41] Wolff, S. J., Lin, S., Faierson, E. J., Liu, W. K., Wagner, G. J., Cao, J. (2017). A framework to link localized cooling and properties of directed energy deposition (DED)-processed Ti-6Al-4V. Acta Materialia, 132, 106117.

[42] Yan, F., Xiong, W., Faierson, E. (2017). Grain structure control of additively manufactured metallic materials. Materials, 10(11), 1260.

[43] Amini, M. and S. Chang, A review of machine learning approaches for high dimensional process monitoring. 2018.

[44] Amini, M. and S. Chang, Process Monitoring of 3D Metal Printing in Industrial Scale. 2018(51357): p. V001T01A035.

[45] Amini, M. and S.I. Chang, MLCPM: A process monitoring framework for 3D metal printing in industrial scale. Computers Industrial Engineering, 2018. 124: p. 322-330.

[46] Imani, F., et al., Layerwise In-Process Quality Monitoring in Laser Powder Bed Fusion. 2018.

[47] Yao, B., et al., Multifractal Analysis of Image Profiles for the Characterization and Detection of Defects in Additive Manufacturing. Journal of Manufacturing Science and Engineering, 2018. 140(3): p. 031014-031014-13.

[48] Imani, F., et al., Process Mapping and In-Process Monitoring of Porosity in Laser Powder Bed Fusion Using Layerwise Optical Imaging. Journal of Manufacturing Science and Engineering, 2018. 140(10): p. 101009101009-14.

[49] Montazeri, M., et al., In-Process Monitoring of Material CrossContamination Defects in Laser Powder Bed Fusion. Journal of Manufacturing Science and Engineering, 2018. 140(11): p. 111001-111001-19.

[50] Sedaghati, A. and H. Bouzary, A study on the effect of cooling on microstructure and mechanical properties of friction stir-welded AA5086 aluminum butt and lap joints. Proceedings of the Institution of Mechanical Engineers, Part L: Journal of Materials: Design and Applications, 2017: p. 1464420717726562.

[51] Igbelina, C., The Synergistic Integration of Mass Customization, Parametric Design and Additive Manufacturing: A Case of Personalized Footwear. 2018 (Doctoral dissertation, The University of Texas at San Antonio).

[52] Taheri, H., Koester, L. W., Bigelow, T. A., Faierson, E. J., Bond, L. J. (2019). In-situ additive manufacturing process monitoring with an acoustic technique: clustering performance evaluation using K-means algorithm. Journal of Manufacturing Science and Engineering, 1-27.

[53] Attoye, S., E. Malekipour, and H. El-Mounayri, Correlation Between Process Parameters and Mechanical Properties in Parts Printed by the Fused Deposition Modeling Process. in Mechanics of Additive and Advanced Manufacturing, Volume 8. 2019. Cham: Springer International Publishing.

[54] Malekipour, E., S. Attoye, and H. El-Mounayri, Investigation of Layer Based Thermal Behavior in Fused Deposition Modeling Process by Infrared Thermography. Procedia Manufacturing, 2018. 26: p. 1014-1022.

[55] Ebrahimpour, A., et al., Experimental Measurement and Numerical Simulation of Temperature Distribution and Thermal History During Friction Stir Welding of Pure Copper Joints. Journal of Mechatronics, 2014. 2(2): p. 113-118.

[56] Malekipour, E., A. Tovar, and H. El-Mounayri. Heat Conduction and Geometry Topology Optimization of Support Structure in Laser-Based Additive Manufacturing. in Mechanics of Additive and Advanced Manufacturing, Volume 9. 2018. Cham: Springer International Publishing.

[57] Yu, Ning. Process parameter optimization for direct metal laser sintering (DMLS). PhD diss., 2005.